counting methods (TR 40–160, 16 bits, Licel, Germany), except 1064 nm (only analog method) [47]. Through different wavelengths in various configurations, which EMORAL is able to measure, it is possible to observe presence of different particles in the atmosphere e.g. small ones such us sulfates and soot, fraction of small-size mineral-dust particles, as well as to some extend also larger particles and hydrometeors such as clouds, ice crystals and hail [48]. The simplest form of the detected Lidar signal is as follows [45]:

$$P(r)=K \cdot O(r) \cdot \beta(r) \cdot T(r) \quad (3)$$

Where:
K is a Lidar system constant, $O(r)$ is a range dependent measurement geometry, both variables result from the design and components of the device. backscattering coefficient at range (r) describes $\beta(r)$, and transmission $T(r)$ describes the losses of the emitted signal. The latter both variables depend on atmospheric conditions during the measurement. The LiDAR equation in a more detailed form reads [45, 48, 49]:

$$P(r) = P_0 \cdot \frac{c\tau}{2} \cdot \eta \cdot A \cdot \frac{O(r)}{r^2} \cdot \beta(r) \cdot \exp\left[-2\int_0^r \alpha(r) \cdot dr\right] + P_{bgr} \quad (4)$$

where:

$$\beta(r)=\beta_{mol}(r)+\beta_{aer}(r) \quad (5)$$

$$\alpha(r)=\alpha_{mol}(r)+\alpha_{aer}(r) \quad (6)$$

P_0 is the average power of a single laser pulse, c is the speed of light, τ is the duration of the laser pulse, η describes the optical efficiency of system components (overall system efficiency) and A is a telescope area. The overlap geometric form factor $O(r)$ determines whether the laser beam is fully detected by the telescope. The raw signal includes background (P_{bgr})solar radiation during daytime and electronic noise. The background is subtracted before starting the signal analysis. The most important variables are extinction coefficient α(r) and backscattering coefficient β(r), by means of which one can determine the type of aerosol particles suspended in the air. Extinction occurs due to scattering and absorption of light by particles and molecules, while backscattering coefficient describes how much light is scattered backwards onto the lidar receiver, and consequently is the basic atmospheric parameter determining the lidar signal strength. Lidar measures total extinction and backscattering coefficients, from which the aerosol extinction and backscattering coefficients (index *aer*) can be calculated by subtracting the molecular (index *mol*) component (usually obtained from radiosounding). Signals collected during laser measurements are automatically processed into a graphic form of quick-looks (fig. 2), which allows assessing the aerosol/cloud atmospheric situation.

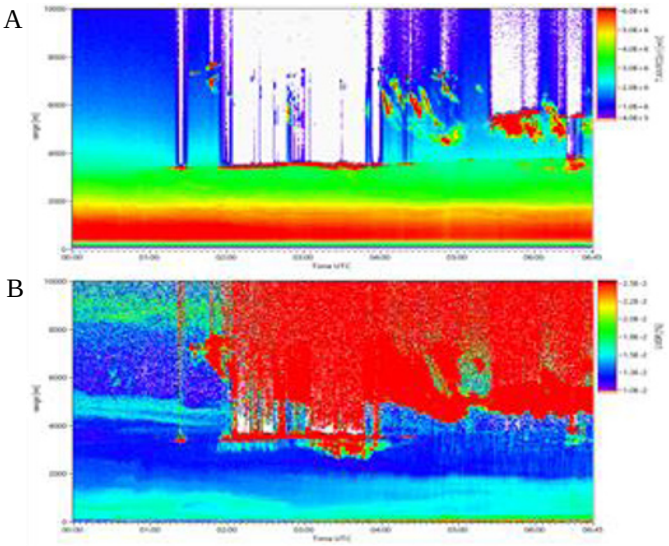

Fig. 2. Backscattering coefficient – background and range corrected signal at the 355 nm – analog sensor (A) and linear volume depolarization ratio at 355 nm (B). The data was obtained on 22.05.2018 00:00–06:45 UTC at the Rzecin peatland.

3.2.2 Sun photometer

A multiband automatic sun photometer CE318 (CIMEL Electronique, France) is the ground based passive remote sensing instrument installed at the Rzecin peatland at a 4 m high tower. It is an autonomous equipment that carries out continuous observations on a fully automatic mode [50].

In principle, this device measures the solar radiation attenuation that is caused by the presence of atmospheric aerosols above the sun photometer.

During a single measurement, the robotic sensor head is aiming at the sun disk and the observations are completed when the path between the sensor and sun is free of clouds. The measurements of the AOT are conducted simultaneously within 9 spectral bands 340, 380, 440, 500, 675, 870, 940, 1020 and 1640 nm [51, 52]. This sun photometer is integrated within the Aerosol Robotic Network (AERONET) and operates under a standardized measurement protocol. This particular instrument is set up to measure both spectral sun and sky irradiances.

The measured values are automatically transmitted and collected in the framework of the AERONET, where the data is processed and presented at the organization's website [51]. The AERONET provides also the standardized calibration procedure for each device to improve the quality of collected data. The sensor characteristics obtained within the calibration process are used for correction of the previously obtained data.

4 Ecosystem measurements

Field measurements of CO_2 uptake are fundamental for the estimation the productivity of the entire ecosystem. Thus, the eddy covariance (EC) technique [37] is applied

to measure the net ecosystem production (NEP) at the Rzecin peatland [38]. The system operates in a continuous mode that basically consists of two devices: the sonic anemometer (R3–50, Gill Ltd., Limington UK) and the H_2O/CO_2 infrared gas analyser (LI–7200, LI–COR, Lincoln USA). Fast and accurate measurements of CO_2 concentrations and vertical wind speed component fluctuations are used for the calculations of net CO_2 flux density using the following formula [53]:

$$F_C = \rho_a \cdot \overline{w' \cdot s'} \quad (7)$$

where:

F_C – net CO_2 flux density [$g \cdot m^{-2} \cdot s^{-1}$]

ρ_a - average dry air density[$g \cdot m^{-3}$],

w' - wind speed vertical component fluctuation [$m \cdot s^{-1}$],

s' – CO_2 mixing ratio (dry air) fluctuation [$g \cdot g^{-1}$].

Both sensors are installed on a 4.5 m tall tower that is located in the central part of the peatland.

The discontinuities in NEP time series are caused either by technical (e.g. lack of power) or methodological (e.g. lack of turbulence) reasons. Thus, the gap filling procedures have been developed in order to achieve temporal continuity of the time series [54].

The Rzecin EC system is enriched with solar radiation and air temperature sensors, as radiative and thermal factors are main determinants of the ecosystem production. Both global and scattered Photosynthetic Photon Flux Density (PPFD) measurements are carried out using the sunshine sensor (BF5, DeltaT, UK) [55]. Additionally, air relative humidity and temperature are measured (HMP, Vaisala, Finland). Nocturnal values of net ecosystem production are used for the parametrization of ecosystem respiration (Reco) [56] determined by air temperature values. This relationship, in combination with NEP values, is finally used for the assessment of the gross ecosystem production (GEP).

5 Instrumental synergies

General idea on instrumental synergies can be assessed by close view on atmospheric situation above the measurement site, which can be characterized on the basis of radar and lidar quick-looks comparison (figs. 1 and 2). Data interpretation can be supported by the analysis of backward-trajectories [57], modeled aerosol observations [58], and global fire data [59]. The analysis of lidar quick-look (fig. 2B) shows highly polarizing layers at a heights of 4.5-5 and 9 km. In addition, the stratification within the boundary layer (due to polarization presence) at 0:00–4:30 UTC is noticeable. This stratification is not observed in backscattering coefficient (fig. 2A). The height of the boundary layer is relatively constant and fluctuates around 2 km. The aerosol concentration in the layer between 4.5 and 5.5 km is decreasing with time. It seems to disappear after cirrus appearance after 4 UTC. The saturation of the signal is also observed (cloud layer consisting of rather large particles, which results in signal attenuated in/above cloud).

The combined analysis of radar and lidar graphs allows to state that clouds have been likely formed on the aerosol layer. It is confirmed by backward-trajectories and modeled aerosol observations (not shown here for brevity), which indicated the occurrence of smoke (fires in Scandinavia) and sulfate (from anthropogenic or biogenic (e.g. marine plankton activity) sources) over the Rzecin peatland around 3 UTC on 22nd of May 2018 at the three height: 2 (top of boundary layer), 5 and 9 km.

Radar quick-looks give an information about the height of the clouds base and top, and its internal structure. Comparison of lidar and radar obtained data, enables to distinguish whether lidar observes very strong aerosol clusters or rather clouds (e.g. between 3:00–4:00 UTC a strongly depolarizing layer at a height of about 3 km is observed and its located right under the cloud base, while it is not found in radar data).

Radar observations provide also information regarding the structure of the cloud droplet movements (up- and down-drafts). The fall of clouds particles between 4:00 and 5:00 UTC is noticed.

The combination of the lidar data with the sun-photometry is crucial for the study of the aerosol optical properties. The derivation of the extinction coefficient at daytime from the lidar data alone is often limited by the high background radiation. The lidar data can be constrained with the photometer column at values to obtain high quality profiling at daytime.

6 Ecosystem modelling and outlook

Although research of peatlands is recognized an important scientific topic due to its sensitivity to climate variability, the impact of air optical properties on peatland ecosystems productivity has been rarely investigated. Recently observed trends of atmospheric optical parameters, e.g. global brightening [60], allows for expecting the linkages between incoming solar radiation and its scattering processes with the intensity of vegetation photosynthesis. Integrated aerosol/cloud and ecosystem studies are crucial for better understanding, parametrization, and consequently the peatlands fate prediction.

In the context of ecosystems, their productivity models consider a plant's canopy as a one solid layer ('big leaf') and this simplified approach results in an overestimation of plant canopy photosynthesis [61]. Two-layer models show better agreement between field measurements and simulated values than a big leaf one and this improvement is achieved by including both shaded leaves and scattered solar radiation [62]. The most complex multilayer models present the best estimation of ecosystem production, whereby they base on the photosynthesis estimation at the each sublayer of the entire plants canopy [63].

The research conducted within the POLIMOS, combines techniques briefly described in the above sections, as applied simultaneously over the Rzecin

peatland. This provides detailed description of both cloud (cloud radar observation) and aerosol (lidar observation) properties, as well as CO_2 uptake (EC and meteorological measurements).

This unique data set serves as the basis for the development the complex model that will comprise both the radiative transfer modelling (RTM) and the ecosystem production modelling (EPM) (fig. 3).

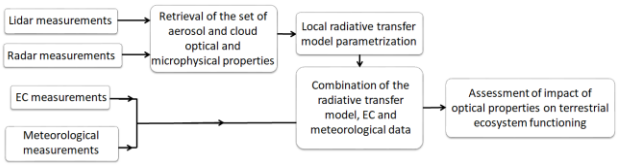

Fig. 3. The block scheme of the research plan.

Generally, EPM estimates direct and scattered radiation fluxes that reach the leafs in the canopy. The upper leafs receive both direct and scattered radiation, while shaded leafs get only the scattered type of solar irradiance. The total canopy CO_2 uptake is the sum of the separated parts of whole vegetation layer. The plant canopy structure applied in EPMs differs from simplified (single layer) to complex (multi-layer) one. Finally, the radiative transfer models provides the assessment of direct and scattered radiation fluxes. These values are used as an input data for ecosystem production model.

Both RTM and EPM parametrization will deliver the quantitative ecosystem production where atmospheric optical properties will be taken into account. Such a complex model will be a useful tool for aerosols and/or clouds effect disentangling from the group of factors that determine the peat vegetation photosynthesis.

The Technical assistance for Polish Radar and Lidar Mobile Observation System (POLIMOS) project is coordinated by the Institute of Geophysics, Faculty of Physics, University of Warsaw and funded by the European Space Agency (ESA-ESTEC) under the Polish Industry Incentive Scheme (PLIIS) with Contract no.4000119961/16/NL/FF/mg.
The core collaborators the POLIMOS projects are University of Warsaw (IG FUW, Poland), Poznan University of Life Sciences (PULS, Poland), Laboratoire Atmosphères, Milieux, Observations Spatiales (LATMOS, France), Ludvig-Maximilians-Universität (LMU-MIM, Germany), University of Granada (Spain), Raymetrics SA (Greece), Licel GmbH (Germany), Innolas-Lasers GmbH (Germany).

References

1. E. Lappalainen, *General review on world peatland and peat resources*, in: E. Lappalainen (ed.) *Global Peat Resources* (International Peat Society and Geological Survey of Finland, Jyska, Finland, 53–5, 1996)
2. S.E. Page, J.O. Rieley, C.J. Banks, Glob. Chang. Biol. **17**, 798–818 (2011)
3. R.S. Clymo, J. Turunen, K. Tolonen, Oikos **81**, 368–388 (1998)
4. L. Bragazza, Glob. Chang. Biol. **14**, 2688–2695 (2008)
5. M. Migliavacca, M. Galvagno, E. Cremonese, M. Rossini, M. Meroni, O. Sonnentag, S. Cogliati, G. Manca, F. Diotri, L. Busetto, A. Cescatti, R. Colombo, F. Fava, U. Morra di Cella, E. Pari, C. Siniscalco, A.D. Richardson, Agric. For. Meteorol. **151**, 1325–1337 (2011)
6. O. Sonnentag, M. Detto, R. Vargas, Y. Ryu, B.R.K. Runkle, M. Kelly, D.D. Baldocchi, Agric. For. Meteorol. **151**, 916–926 (2011)
7. O. Sonnentag, K. Hufkens, C. Teshera-Sterne, A.M. Young, M. Friedl, B.H. Braswell, T. Milliman, J. O'Keefe, A.D. Richardson, Agric. For. Meteorol. **152**, 159–177 (2012)
8. W.L. Bauerle, R. Oren, D.A. Way, S.S. Qian, P.C. Stoy, P.E. Thornton, J.D. Bowden, F.M. Hoffman, R.F. Reynolds, Proc. Natl. Acad. Sci. **109**, 8612–17 (2012)
9. B. Robroek, M.G.C. Schouten, J. Limpens, F. Berendse, H. Poorter, Glob. Chang. Biol. **15**, 680–691 (2009)
10. A. Yurova, A. Wolf, J. Sagerfors, M. Nilsson, J. Geophys. Res. **112**, G02025 (2007)
11. B.N. Sulman, A.R. Desai, N.Z. Saliendra, P.M. Lafleur, L.B. Flanagan, O. Sonnentag, D.S. Mackay, A.G. Barr, G. van der Kamp, Geophys. Res. Lett. **37**, L19702 (2010)
12. A. Lindroth, M. Lund, M. Nilsson, M. Aurela, T.R. Christensen, T. Laurila, J. Rinne, T. Riutta, J. Sagerfors, L. Stro¨M, J.P. Tuovinen, T. Vesala, Tellus B **59**, 812–25 (2007)
13. M. Lund, P.M. Lafleur, N.T. Roulet, A. Lindroth, T.R. Christensen, M. Aurela, B.H. Chojnicki, L.B. Flanagan, E.R. Humphreys, T. Laurila, W.C. Oechel, J. Olejnik, J. Rinne, P. Schubert, M.B. Nilsson, Global Change Biol. **16**, 2436–2448 (2010)
14. P. McVeigh, M. Sottocornola, N. Foley, P. Leahy, G. Kiely, Agric. For. Meteorol. **194**, 8–19 (2014)
15. L.M. Mercado, N. Bellouin, S. Sitch, O. Boucher, C. Huntingford, M. Wild, P.M. Cox, Nature **458**, 1014–1017 (2009)
16. O. Urban, D. Janous, M. Acosta, R. Czerny, I. Markova, M. Navratil, M. Pavelka, R. Pokorny, M. Sprtova, R. Zhang, V. Spunda, J. Grace, M.V. Marek, Glob. Chang. Biol. **13**, 157–168 (2007)
17. S. Dengel, J. Grace, Oecologia **164**, 797–808 (2010)
18. K.D. Kanniah, J. Beringer, P. North, L. Hutley, Progress Phys. Geogr. **36**, 209–237 (2012)
19. D.Y. Hollinger, F.M. Kelliher, J.N. Byers, J.E. Hunt, T.M. McSeveny, P.L. Weir, Ecology **75**, 134–150 (1994)
20. K. Harenda, M. Piątyszek, B.H. Chojnicki, Acta Agroph. **22**, 387–395 (2015)
21. L. Gu, D. Baldocchi, S.B. Verma, T.A. Black, T. Vesala, E.M. Falge, P.R.J. Dowty, Geophys. Res. **107** (2002)

22. Y. Zhou, X. Wu, W. Ju, J.M. Chen, S. Wang, H. Wang, W. Yuan, T.A. Black, R. Jassal, A. Ibrom, S. Han, J. Yan, H. Margolis, O. Roupsard, Y. Li, F. Zhao, G. Kiely, G. Starr, M. Pavelka, L. Montagnani, G. Wohlfahrt, P. D'Odorico, D. Cook, M.A. Arain, D. Bonal, J. Beringer, P.D. Blanken, B. Loubet, M.Y. Leclerc, G. Matteucci, Z. Nagy, J. Olejnik, K.T. Paw U, A. Varlagin, J. Geophys. Res. Biogeosci. **121**, 1045–1072 (2016)
23. O. Urban, K. Klem, A. Ac, K. Havrankova, P. Holisova, M. Navratil, M. Zitova, K. Kozlova, R. Pokorny, M. Sprtova, I. Tomaskova, V. Spunda, J. Grace, Funct. Ecol. **26**, 46–55 (2012)
24. F. Charbonnier, G. Maire, E. Dreyer, F. Casanoves, M. Christina, J. Dauzat, J.U.H. Eitel, P. Vaast, L.A. Vierling, O. Roupsard, Agric. For. Meteorol. **181**, 152–169 (2013)
25. A.M.R. Petrescu, A. Lohila, J.-P. Tuovinen, D.D. Baldocchi, A.R. Desai, N. T. Roulet, T. Vesala, A.J. Dolman, W.C. Oechel, B. Marcolla, T. Friborg, J. Rinne, J.H. Matthes, L. Merbold, A. Meijide, G. Kiely, M. Sottocornola, T. Sachs, D. Zona, A. Varlagin, D.Y.F. Lai, E. Veenendaal, F.-J.W. Parmentier, U. Skiba, M. Lund, A. Hensen, J. van Huissteden, L.B. Flanagan, N.J. Shurpali, T. Grünwald, E.R. Humphreys, M. Jackowicz–Korczyński, M.A. Aurela, T. Laurila, C. Grüning, A.R. Chiara, C.A.R. Corradi, A.P. Schrier–Uijl, T.R. Christensen, M.P. Tamstorf, M. Mastepanov, P.J. Martikainen, S.B. Verma, C. Bernhofer, A. Cescatti, Proc. Natl. Acad. Sci. **112**, 4594–4599 (2015)
26. I.S. Stachlewska, O. Zawadzka, R. Engelmann, Remote Sens. **9** (2017)
27. K. Markowicz, *Metody pomiaru optycznych właściwości aerozolu atmosferycznego*, in: K. Juda-Rezler, B. Toczko (ed.), *Pyły drobne w atmosferze: Kompendium wiedzy o zanieczyszczeniu powietrza pyłem zawieszonym w Polsce* (Biblioteka Monitoringu Środowiska, Warszawa, 106–121, 2016)
28. O. Boucher, D. Randall, P. Artaxo, C. Bretherton, G. Feingold, P. Forster, V.-M. Kerminen, Y. Kondo, H. Liao, U. Lohmann, P. Rasch, S.K. Satheesh, S. Sherwood, B. Stevens and X.Y. Zhang, *Clouds and Aerosols*, in: T.F. Stocker, D. Qin, G.-K Plattner, M. Tignor, S.K. Allen, J. Boschung, A. Nauels, Y. Xia, V. Bex and P.M. Midgley (ed.), *Climate Change 2013: The Physical Science Basis. Contribution of Working Group I to the Fifth Assessment Report of the Intergovernmental Panel on Climate Change* (Cambridge University Press, Cambridge, United Kingdom and New York, NY, USA, 2013)
29. E.J. Freney, K. Adachi, P.R. Buseck, J. Geophys. Res. **115**, D19210 (2010)
30. J.W. Fan, J. M. Comstock, M. Ovchinnikov, Environ. Res. Lett. **5** (2010)
31. R. Wood, J. Atmos. Sci. **64**, 2657–2669 (2007)
32. R.A. Kahn, Surv. Geophys. **33**, 701–721 (2012)
33. G. Pappalardo, A. Amodeo, A. Apituley, A. Comeron, V. Freudenthaler, H. Linné, A. Ansmann, J. Bösenberg, G. D'Amico, I. Mattis, L. Mona, U. Wandinger, V. Amiridis, L. Alados–Arboledas, D. Nicolae, M. Wiegner, Atmos. Meas. Tech. **7**, 2389–2409 (2014)
34. J. Fuchs, J. Cermak, Remote Sens. **7**, 4178–4190 (2015)
35. Y.J. Kaufman, D. Tanré, O. Boucher, Nature **419,** 215–223 (2002)
36. G. Pappalardo, J. Bösenberg, A. Ansmann, D. Balis, C. Böckmann, A. Chaikovsky, A. Comeron, R. Eixmann, I.V. Grigorov, A. Hågård, V. Mitev, S. Nickovic, A. Papayannis, J. Pelon, M.R. Perrone, D. Resendes, V. Rizi, V. Simeonov, P. Sobolewski, N. Spinelli, T. Trickl, G. Vaughan, M. Wiegner, M. Zavrtanik, *Aerosol Lidar measurements in the framework of EARLINET* (2nd Symposium on Lidar Atmospheric Applications, Session 5, Lidar networks and Autonomous systems (5.1), 2005)
37. M. Aubinet, T. Vesala, D. Papale (ed.), *Eddy covariance: A Practical Guide to Measurement and Data Analysis* (Springer Atmospheric Sciences, p. 438, 2012)
38. B.H. Chojnicki, M. Urbaniak, D. Józefczyk, J. Augustin, J. Olejnik, *Measurements of gas and heat fluxes at Rzecin wetland*, in: T. Okruszko, E. Malby, J. Szatylowicz, D. Swiatek, W. Kotowski (ed.), *Wetlands: Monitoring: Monitoring, Modeling and Menagement* (Taylor & Francis Group, London, England, 125–131, 2007)
39. F. Ulaby, D.G. Long, *Microwave Radar and Radiometric Remote Sensing* (Ann Arbor, Michigan, University of Michigan Press, 2014)
40. J. Delanoë, A. Protat, J.-P. Vinson, W. Brett, C. Caudoux, F. Bertrand, J. Parent du Chatelet, R. Hallali, L. Barthes, M. Haeffelin, J.-C. Dupont, J. Atmospheric Oceanic Technology **33**, 1023–1038 (2016)
41. *World Meteorological Organization. International Cloud Atlas. General classification of meteors – Hydrometeors* (Available online: https://cloudatlas.wmo.int/, accessed on 11 April 2018)
42. *American Meteorological Society. Glossary of Meteorology. Radar reflectivity factor* (Available online: http://glossary.ametsoc.org/wiki/Radar_reflectivity_factor, accessed on 15 July 2018)
43. A. Kardaś, *Badanie optycznych i fizycznych własności aerozolu atmosferycznego i cząstek chmurowych na podstawie pomiarów teledetekcyjnych* (Rozprawa doktorska, 2013)
44. D. Balis, V. Amiridis, S. Kazadzis, A. Papayannis, G. Tsaknakis, S. Tzortzakis, N. Kalivitis, M. Vrekoussis, M. Kanakidou, N. Mihalopoulos,

G. Chourdakis, S. Nickovic, C. Pérez, J. Baldasano, M. Drakakis, Annales Geophysicae **24**, 807–821 (2006)

45. U. Wandinger, *Introduction to Lidar*, in: C. Weitkamp (ed.), *Lidar* (Springer New York, **102**, 1–18, 2005)
46. L. Belegante, J.A. Bravo–Aranda, V. Freudenthaler, D. Nicolae, A. Nemuc, D. Ene, L. Alados-Arboledas, A. Amodeo, G. Pappalardo, G. D'Amico, F. Amato, R. Engelmann, H. Baars, U. Wandinger, A. Papayannis, P. Kokkalis, S.N. Pereira, Atmos. Meas. Tech. **11**, 1119–1141 (2018)

    DOI: 10.5194/amt-11-1119-2018
47. Raymetrics S.A., *LR321–D300 Raman Depolarization LIDAR: User Manual* (2017)
48. Raymetrics S.A., *Lidar Analysis: User Manual* (2018)
49. J.D. Vande Hey, *Theory of Lidar*, in: *A Novel Lidar Ceilometer* (Springer International Publishing Switzerland, 23–41, 2015)
50. C. Pérez, S. Nickovic, J.M. Baldasano, M. Sicard, F. Rocadenbosch, V.E. Cachorro, J. Geophys. Res. **111** (2006)
51. A. Smirnov, B.N. Holben, T.F. Eck, O. Dubovik, I. Slutsker, Remote Sens. Environ. **73**, 337–349 (2000)
52. B.N. Holben, T.F. Eck, I. Slutsker, D. Tanre, J.P. Buis, A. Setzer, E. Vermote, J.A. Reagan, Y.J. Kaufman, T. Nakajima, F. Lavenu, I. Jankowiak, A. Smirnov, Remote Sens. Environ. **66**, 1–16 (1998)
53. E.K. Webb, G. Pearman, R. Leuing, Q. J. R. Meteorol. Soc. **106**, 85–100 (1980)
54. M. Reichstein, E. Falge, D. Baldocchi, D. Papale, M. Aubinet, P. Berbigier, C. Bernhofer, N. Buchmann, T. Gilmanov, A. Granier, T. Grünwald, K. Havránkov, H. Ilvesniemi, D. Janous, A. Knohl, T.Laurila, A. Lohila, D. Loustau, G. Matteucci, T. Meyers, Glob. Chang. Biol. **11**, 1424–1439 (2005)
55. J. Wood, T. Muneer, J. Kubie, J. Sol. Energy Eng. **125**, 1–6 (2003)
56. J. Lloyd, J.A. Taylor, Functional Ecology **8**, 315–323 (1994)
57. R.R. Draxler, G.D. Rolph, *HYSPLIT (HYbrid Single-Particle Lagrangian Integrated Trajectory)*, Model access via NOAA ARL READY Website, NOAA Air Resources Laboratory (Silver Spring, MD, USA, 2010, Available online: https://www.ready.noaa.gov/HYSPLIT.php)
58. P. Lynch, J.S. Reid, D.L. Westphal, J. Zhang, T.F. Hogan, E.J. Hyer, C.A. Curtis, D.A. Hegg, Y. Shi, J.R. Campbell, J.I. Rubin, W.R. Sessions, F.J. Turk, A.L. Walker, Geosci. Model Dev. **9**, 1489–1522 (2016),

    Available online: https://www.nrlmry.navy.mil
59. *Global Fire Maps*, (Available online: https://lance.modaps.eosdis.nasa.gov/cgi-bin/imagery/firemaps.cgi, accessed on 15 July 2018)
60. M. Kleniewska, B.H. Chojnicki, M. Acosta, Meteorol. Hydrolo. Water Manage. **4**, 35–40 (2016)
61. D.G.G. De Pury, G.D. Farquhar, Plant Cell Environ. **20**, 537–557 (1997)
62. L. Mercado, J. Lloyd, F. Carswell, Y. Malhi, P. Meir, A.D. Nobre, Acta Amazon. **36**, 69–82 (2006)
63. A. Knohl, D.D. Baldocchi, J. Geophys. Res. **113** (2008)